RESEARCH ARTICLE

Ecological environmental quality evaluation based on multi-source remote sensing technology

Tianjiao Dang*

Shaanxi Fashion Engineering University, Xi'an, Shaanxi, China.

Received: May 29, 2025; **accepted:** October 15, 2025.

Ecological environment (ECO) quality evaluation technology plays an important guiding role in regional economic development and environmental quality. This research proposed an ECO quality evaluation model that combined multi-source remote sensing (MSRS) technology and principal component analysis (PCA) method to improve ECO quality effect. The model applied remote sensing images to obtain the required component index data, introduced PCA method, coupled four index information of greenness, wetness, dryness, and heat, and carried out environmental evaluation through remote sensing ecological index (RSEI). The results showed that the proposed model demonstrated the most significant advantage of monitoring the specific ECO status of the area in a long time series compared with other individual models including remote sensing (RS), MSRS, and PCA. The further evaluation of the ECO quality of the area showed that the effect of the proposed model reached more than 78 points, exceeding other existing models. The proposed ECO quality evaluation model combining MSRS technology and PCA method had certain practical effects and could provide reliable data support in subsequent ECO quality evaluation.

Keywords: multi-source; remote sensing; ecological environment; mass; evaluation.

***Corresponding author:** Tianjiao Dang, Shaanxi Fashion Engineering University, Xi'an, Shaanxi, China. Email: dtj13571952473@163.com.

Introduction

Global climate change has had a profound impact on the ecological environment (ECO), exacerbating various ecological problems such as drought, soil erosion, glacier melting, sharp decline in biodiversity, and air pollution due to the combined effects of climate and human activities. Therefore, it is particularly important to carry out long-term and large-scale ECO quality monitoring. The overall evaluation of ECO quality helps to determine the current state of sustainable development in the study area and relies on structured, semi-structured, and unstructured data analysis, as well as natural, social, and economic multi-faceted datasets. Various special evaluations have been developed including ecological health, ecological vulnerability, and ecological risk with the evaluation level covering from qualitative description to quantitative analysis. The common methods include analytic hierarchy process, ecological footprint method, and artificial neural network evaluation method [1]. Remote sensing technology (RS) has been widely used in regional ECO quality dynamic monitoring. Remote sensing ecological index (RSEI) is constructed by using principal component analysis (PCA) method to select four ecological elements closely related to human beings, which can efficiently and

objectively reflect the dynamic changes of regional ECO quality and have been widely promoted in ECO quality evaluation [2].

Previous research divided ECO quality evaluations into ECO quality status, ECO quality prejudgment, and ECO impact aspects [3]. ECO quality evaluation mainly establishes an index system and chooses an appropriate evaluation method. There are two main criteria for constructing an indicator system, which include the selections based on subjectivity and the natural environment. Jia *et al*. analyzed indicators from the perspectives of climate, vegetation, soil, and hydrological quality, while other researchers incorporated socioeconomic and ecological environmental quality into their models based on the natural environment, socioeconomic factors, and environmental pollution [4]. Hong *et al*. constructed evaluation indexes from three dimensions of pressure, state, and response to comprehensively evaluate ECO quality based on multi-source remote sensing data and found that the selected indexes were highly subjective [5]. In recent years, more scholars tend to use RS to select indexes objectively. Liu *et al*. applied the grey slope correlation method to evaluate the quality status of ECO and established the grey slope correlation model for quantitative calculation [6]. Wang *et al*. used comprehensive index method, analytic hierarchy process, and backpropagation (BP) neural network analysis model to evaluate ECO quality [7]. Liu *et al*. used interval analytic hierarchy process (IAHP) and entropy method to determine the weight value and AHP to evaluate the change of ECO quality [8]. To quantitatively evaluate the quality of ECO in arid areas, Wu *et al*. constructed the early dry RSEI (ARSEI) for arid areas, which combined the information of greenness, wetness, salinity, heat, and land degradation [9]. Tian *et al*. constructed a new RSEI by introducing PM2.5 indicators to evaluate the change of ecological quality, which provided a new method for urban ECO monitoring, especially in exploring the impact of air quality on ECO [10]. Three methods are used for weight determination including subjective weight determination, objective weight determination, and learning weight determination. Subjective weight determination is based on the subjective judgment of individuals or experts, which is simple and fast but is greatly influenced by subjectivity, requires high expert experience and has low reliability. The results of objective weight determination are more objective but may have problems such as weight distortion and weight value that cannot be directly determined [11]. Learning weight determination is through machine learning algorithms or statistical models based on historical data or known information, mainly including neural networks and decision trees. This method uses the relationship and pattern between data to automatically learn the allocation of weights, thus reducing the influence of subjective factors and improving the objectivity and accuracy of evaluation results. Therefore, introducing or combining learning methods with objective evaluation methods has become a hot spot in current ecological evaluation research [12]. Yang *et al*. used remote sensing and geographic information system (GIS) to monitor water quality parameters [13], while Wang *et al*. used NASA's moderate resolution imaging satellite data (MODIS) to calculate the annual aerosol optical depth (AOD) and measure PM2.5 concentration on the ground and evaluated the particulate air quality in different parts of cities around the world [14]. Xu *et al*. also used remote sensing data and GIS to invert landscape-level environmental indicators for quantitative estimation of coastal and estuarine habitat trends [15], while Ghorbanian *et al*. monitored the status of shrimp farming based on remote sensing and GIS to accurately predict water quality parameters in the context of sustainable shrimp farming [16]. The information obtained by aerial and satellite remote sensing can objectively reflect the shape, structure, and spatial relationship of mining area scenery, and comprehensively reflect various environmental information such as atmosphere, water body, soil, and vegetation. Duan *et al*. tried to expand the scope of monitoring targets including mining area building classification, subsidence area classification, land use classification, water

pollution classification, vegetation classification, surface collapse, karst subsidence column, solid waste, and other aspects [17]. Ren *et al*. proved that RS had good effects and application prospects in ecological restoration construction by using high-resolution remote sensing images [18]. Tang *et al*. identified the characteristics of mine geological environment and ecological restoration changes to further prove the objectivity, accuracy, and the effectiveness of satellite remote sensing monitoring [19]. With the progress of unmanned aerial vehicle (UAV) systems and the increase of sensor types, UAV RS has been widely used and shows a good application prospect. Li *et al*. has achieved several results in the application of UAV RS in ecological restoration, covering the fields of geological disaster investigation, land remediation, soil and water conservation projects, and monitoring and management of animal and plant resources [20].

RS shows great application potential in ECO monitoring. This study proposed an ECO quality evaluation model combining multi-source remote sensing (MSRS) technology and PCA method to improve the objectivity and accuracy of evaluation by efficiently integrating key indicators including greenness, humidity, dryness, and heat. The proposed model could dynamically reveal the regional ECO quality status, provide scientific basis for evaluating the sustainable development status of the research area, and compensate for the subjectivity and limitations of traditional methods in data acquisition and weight allocation.

Materials and methods

Data collection

The data of four core ecological element indicators of greenness including normalized vegetation index, reflecting vegetation coverage (NDVI), humidity representing soil and open water humidity based on canopy transformation (WET), dryness combining bare soil index and building index to indicate surface drying degree (NDBSI), and heat including surface temperature, revealing thermal environmental effects (LST) were collected through multi-source remote sensing technology and normalized to eliminate the dimension difference. The principal component analysis (PCA) method was introduced for dimension reduction coupling. The first principal component (PC1) was extracted as the initial ecological index (RSEI-0), and then the final RSEI value ranged from 0 to 1 was obtained through standardization treatment, which objectively and dynamically reflected the regional ecological environment quality level with the higher the value, the better the ecological situation.

Model construction

U-Net is a convolutional neural network model, which can support a small amount of data to train the model with fast image segmentation speed, classification of each pixel, and higher segmentation accuracy. The RIAU-Net network proposed in this study added attention gate (AGs) mechanism based on U-Net, which had the advantages of U-Net network and could make the model pay more attention to the types of features needed in the research. Multi-temporal and multi-channel data of the region were employed as data input. RIAU-Net network was used for ECO recognition with AGs for semantic segmentation and image classification. The shrinkage path of RIAU-Net consisted of two 3 × 3 convolution layers, a linear correction unit (ReLU), and a 2 × 2 maximum pooling layer. The contraction path was a down sampling operation with the stride length of 2. During the down sampling process, features of image position and semantic information were extracted. Feature map of the corresponding layer of the jump connection related to the feature map of the previous layer input of the upsampling layer. After converting the previous layer and the current layer to the same size, they were added and followed by a series of calculations of ReLU and Sigmoid. Resample was performed to obtain the attention coefficient. The concatenation layer was obtained by multiplying the current layer to realize the RIAU - Net network attention

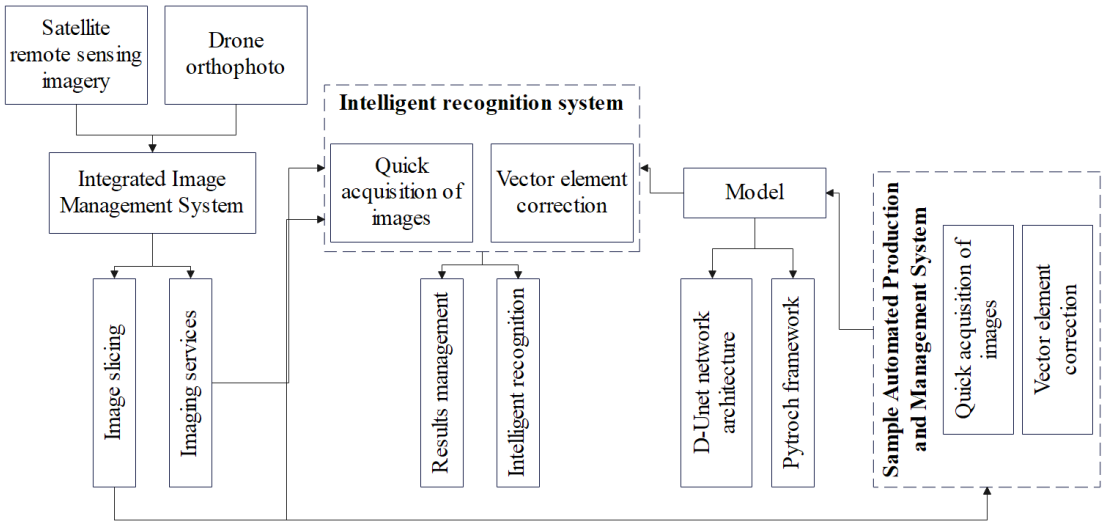

Figure 1. Overall remote sensing image intelligent recognition system design.

on the target area, thereby improving the network's ability to extract salient regional features. Point cloud feature extraction and topology construction technology were used to construct the top and facade models of the building, respectively. The vector features extracted from the oblique image were used to constrain the boundary rules of the top and facade of the building due to the serious aliasing problem of the point cloud boundary. The topology reconstruction and verification of the complex roof were carried out based on the semi-automatic interactive mode of "feature point and line interactive acquisition-interactive topology editing-3D model" of oblique multi-view images. The automatic texture mapping of oblique images was then performed, which mainly included model patch decomposition, optimal texture selection, and multi-view texture fusion. The remote sensing image intelligent recognition system was proposed based on GIS service (Figure 1), which included comprehensive management of image data by using database and file storage technology for image files according to topics and histories and GIS server for image services publishing; automated production of sample data sets by loading maps on demand through HTTP protocol and building an automatic sample production and management system based on the technologies of rapid image acquisition and vector element deviation correction based on GIS service to automatically obtain sample pictures and draw sample feature range to build a sample library; model training that included the construction of D-Unet model using deep learning framework and reading the samples in the sample library for model training; image recognition including loading the map on demand through HTTP protocol, defining the detection range, and training D-Unet model to detect the image according to the detection range. Through the image vector feature correction technology based on GIS service, the detection results were extracted into vector types with real geographical coordinates, and the persistent storage management and visual presentation were then carried out.

Experimental environments and indicator determinations

The development environment used for this research included PyCharm2021.2.3 (https://www.jetbrains.com/pycharm/) and PyTorch1.12.1 (https://pytorch.org/). The model training was done on an NVIDIAA10GPU (https://www.nvidia.com/) with 24 GB of video memory. The total number of training iterations (Epoch) was set to 400. The model was optimized by using Adam optimization algorithm. During

the training process, the initial learning rate (LR) was set to 0.000001 with the Batch size of 16. After the normalization of greenness (NDVI), wetness (WET), dryness (NDBSI), and heat (LST) data of the study area from 2004 to 2024, the PCA module of Google Earth Engine (GEE) cloud platform (https://earthengine.google.com/) was used to perform PCA on the four indicators. The image pixel values were calculated using spatial data processing library (https://gdal.org/) and Landsat series satellite images including TM/OLI sensors to obtain near-infrared (NIR) and red (Red) reflectance data. The Google earth engine platform was then used for radiometric calibration, atmospheric correction, and normalization processing. The NDVI mean and standard deviation of the study area were calculated. The humidity component was calculated through the tassel transformation formula by using the reflectance of the blue, green, red, near infrared, and shortwave infrared bands from Landsat 5 TM/8 OLI images. Combined with the bare soil index (SI) and building index (IBI), a dryness index (NDBSI) was constructed. The brightness temperature formula and surface temperature formula were applied for inversion and the calculation of the mean values of each period after normalization based on the radiation calibration value and calibration coefficient of Landsat thermal infrared band. The normalized indicators were merged into a multidimensional dataset on the GEE platform. The built-in PCA module automatically calculated the eigenvectors, eigenvalues, and contribution rates of each principal component, and extracted the weight distribution results of PC1 to PC4. The output of PC1 by PCA was used as the initial ecological index RSEI0, which was converted into a 0 - 1 range value through a standardized formula. The minimum, maximum, mean, and standard deviation of RSEI for five periods were then calculated.

Model evaluation

Ten (10) sets of expert evaluation experiments were conducted to compare the effectiveness of traditional remote sensing (RS), MSRS technology, PCA technology, and proposed MSRS-PCA model in ECO quality evaluation. Experts independently evaluated the accuracy and temporal consistency of the ecological quality grading output by the models. An average of 10 results were taken. Based on the vegetation coverage (verified NDVI), soil moisture (verified WET), and surface temperature data measured on the ground, regression analysis was conducted with the results of traditional RSEI, TNN-RSEI, and MSRS-PCA models to calculate the coefficient of determination (R^2) and mean square root error (RMSE). When calculating accuracy and stability data, the seasonal deviation elimination rate (SDER) was verified by multi-temporal remote sensing data as follows.

SDER = 1-|difference between dry season and rainy season results|/mean value

The spatial consistency adopted the correlation coefficient between mountainous and plain areas. Cloud and fog interference loss rate was the proportion of invalid pixels. The temperature inversion error was obtained by comparing the measured values of ground thermometers. All indicators were averaged after 3 repeated measurements.

Results and discussion

Determination of indicators using proposed model

After normalizing the data of greenness (NDVI), wetness (WET), dryness (NDBSI), and heat (LST) in the study area from 2004 to 2024, PCA was performed on the four indicators by using the PCA module of Google earth engine cloud platform (Table 1). The results of NDVI showed that the average NDVI values were 0.7673 ± 0.2346, 0.6653 ± 0.2346, 0.7088 ± 0.2327, 0.7039 ± 0.2079, 0.8474 ± 0.1762 for 2004, 2009, 2014, 2019, 2024, respectively. The overall trend demonstrated a decrease followed by an increase with significant deterioration from 2004 to 2009 with an average decrease of 13.3% and then gradually improving after 2014 and reaching

Table 1. PCA results of RSEI component indicators.

Year	Principal component	Greenness	Wetness	Dryness	Land surface temperature	Eigenvalues	Contribution rate (%)
2004	PC1	0.9056	0.0207	-0.3990	-0.0226	0.0413	78.4872
	PC2	0.2191	-0.2360	0.4381	0.8273	0.0075	14.3748
	PC3	0.2690	-0.4906	0.6154	-0.5370	0.0029	5.4351
	PC4	0.1996	0.8266	0.5003	-0.0820	0.0004	0.7029
2009	PC1	0.8801	0.1730	-0.4190	-0.0097	0.0141	65.8053
	PC2	0.3672	-0.5290	0.5645	0.4968	0.0045	21.0969
	PC3	0.2051	-0.3893	0.2505	-0.8507	0.0023	10.6623
	PC4	0.1693	0.7203	0.6505	-0.0972	0.0003	1.4355
2014	PC1	0.8754	0.0617	-0.4330	-0.1500	0.0092	65.3103
	PC2	0.2459	-0.2483	0.6797	0.6292	0.0032	22.7106
	PC3	-0.3769	0.2421	-0.4682	0.7485	0.0014	9.7812
	PC4	-0.1062	-0.9253	-0.3338	0.0369	0.0002	1.1979
2019	PC1	0.6582	0.2833	-0.6544	-0.1957	0.0196	64.1520
	PC2	0.7138	-0.4217	0.5408	-0.0185	0.0073	23.9382
	PC3	-0.1513	-0.0830	0.1020	-0.9695	0.0032	10.3851
	PC4	-0.1206	-0.8457	-0.4990	0.0387	0.0002	0.5346
2024	PC1	0.6654	0.1631	-0.7136	-0.0395	0.0211	77.6259
	PC2	0.7297	-0.2387	0.6245	0.0254	0.0054	20.1366
	PC3	-0.0040	0.0394	0.0600	-0.9874	0.0003	0.9603
	PC4	-0.0696	-0.9460	-0.2780	-0.0544	0.0001	0.2772

its peak in 2024 with an increase of 10.4% compared to 2004. The results indicated that the regional vegetation coverage was damaged by development activities in the early stage and significantly restored due to ecological restoration in the later stage. The early deforestation and mining development had a strong destructive effect on the surface vegetation, resulting in a low distribution of NDVI index. As society's awareness of ECO protection continued to increase, and the region continued to promote ecological restoration and mine remediation, NDVI demonstrated an upward improvement since 2014.

The results of WET showed that the average values of the five periods were 0.4712, 0.6346, 0.5316, 0.6366, and 0.9148 in 2004, 2009, 2014, 2019, and 2024, respectively. The humidity level fluctuated significantly with the overall change showing a trend of first rising, then falling, and then rising again. The lowest WET was observed in 2004, which was affected by drought. It showed an upward trend from 2009 to 2019 and reached a peak in 2024 due to floods with an increase of 94.1% compared to 2004. The overall humidity significantly increased over the past 20 years, but the interannual variability also increased with the standard deviation expanded by 28.9%, reflecting the intensified impact of climate anomalies.

NDBSI reflected the degree of surface exposure and hardening with values ranging from 0 (low dryness) to 1 (high dryness), which was dominated by changes in the underlying surface. The exposed and hardened surface hindered the normal circulation of water and made the surface in some areas showing dry characteristics. Therefore, the underlying surface was the key factor affecting dryness. From 2004 to 2024, regional dryness continued to increase due to soil erosion and urbanization, but the specific mean value was not explicitly listed. The analysis indicated that the combination of building index (IBI) and bare soil index (SI) effectively quantified

the "drying" effect, and standardization ensured data comparability by normalizing all values to the 0 - 1 range. The mean values of LST in the five periods were 0.3326, 0.3307, 0.3762, 0.3802, and 0.5049 in 2004, 2009, 2014, 2019, and 2024, respectively.

The average heat index in 2004, 2009, 2014, 2019, and 2024 were 0.5683, 0.5702, 0.5445, 0.6386, and 0.5881, respectively. The heat index demonstrated a phased increase of 14.3% from 2004 to 2019 due to the intensification of urban heat island effect caused by urbanization followed by slightly 5.2% decline in 2024 compared to 2019. However, it was overall increased by 51.8% over the past 20 years, which might be that the urban area had been continuously expanded, and the land surface temperature island effect had been strengthened due to the advancement of urbanization, indicating that urban expansion had a sustained impact on the thermal environment.

The PCA results showed that the sum of the characteristic contribution rates of PC1 and PC2 of the five component indicators in the study area in 2004, 2009, 2014, 2019 and 2024 were all over 85%, and the weighted superposition analysis of the first two principal components expressed the characteristics of the four component indicators to the greatest extent. PC1 concentrated the characteristics of each component index to the maximum extent and could be used to calculate RSEI and reflect the ECO quality status. According to the contribution rate of different component indexes in the principal component, more objective results were obtained by automatically screening indexes, thus ensuring the objectivity of index weights in index integration. The characteristic vector results of each component index obtained by PCA with the indexes of negative and positive values in PC1 were dryness, heat and wetness, and greenness, respectively. In further analysis of the principal components of PC2, PC3, and PC4, the results showed that the eigenvectors of the four indexes had no regularity, and their values were positive and negative disordered. According to the regular characteristics of the four indicators in PC1, it was further indicated that greenness and wetness played a positive role in RSEI, which positively improved the quality of ECO. On the contrary, the negative effect of negative heat and dryness in RSEI had an inhibitory effect on the improvement of ECO quality. Those results were in line with reality. This study confirmed that PC1 could be well used to construct the initial RSEI RSEI0, while PC2, PC3, and PC4 were difficult to use in the calculation of RSEI0 because the index eigenvectors did not have the regularity in line with the actual situation. The mean RSEI values of five different periods were 0.763, 0.729, 0.726, 0.703 and 0.699, respectively. The regional overall ECO quality was directly related to the mean value of the indicators. Comparing the overall evolution trend of RSEI in the past 20 years, the overall value was in a high range and showed a slow downward trend, which meant that the ECO quality in this region was good, but there was a certain downward trend.

Validation of proposed model

The effects of the proposed model and other models in ECO quality evaluation were compared. The results showed that the average model evaluation scores of RS, MSRS technology, and PCA technology were 67.36, 73.09, and 68.00, respectively, while the average score of proposed model was 80.60, which verified that the proposed model in this research had better performance than existing models (Table 2). The NDVI correlation of RSEI method was 0.78, while the NDVI correlation of TNN-RSEI method was 0.82, which was slightly higher than that of RSEI method. The NDVI correlation of MSRS-PCA method was 0.89, which was the highest among the three methods, indicating that the correlation between MSRS-PCA method and NDVI was the strongest, while the correlation between RSEI method and NDVI was the weakest.

The humidity correlations of RSEI, TNN-RSEI, MSRS-PCA methods were 0.65, 0.73, 0.81, respectively. MSRS-PCA method performed the

Table 2. Comparison of ECO quality evaluation methods.

	RS	MSRS technology	PCA	The proposed model
1	67.29	76.81	66.19	79.30
2	65.08	73.58	69.88	83.29
3	67.01	71.52	67.76	82.18
4	63.48	71.76	65.43	78.56
5	70.79	71.29	65.22	79.52
6	67.58	76.78	68.93	79.89
7	67.11	76.65	68.86	79.23
8	70.06	69.05	69.86	80.18
9	65.21	70.67	68.32	81.98
10	70.02	72.82	69.51	81.90

best in the aspect of humidity correlation, while the performance of RSEI method was relatively poor.

The thermal errors of RSEI, TNN-RSEI, MSRS-PCA methods were 2.8°C, 2.1°C, 1.5°C, indicating that the error of MSRS-PCA method in thermal prediction was the smallest and the accuracy was the highest, while the error of RSEI method was the largest and the accuracy was the lowest. Overall, the MSRS-PCA method performed best in terms of NDVI correlation, humidity correlation, and heat error, and its correlation was the highest and error was the lowest. Multi-source data fusion reduced the average annual PCA weight allocation error to 4.7%, significantly lower than 9.6% of single source data. Through multi-source data collaboration and dynamic PCA weight optimization, this proposed model solved the problems of traditional methods being limited by single-period data and improved methods relying on fixed annual averages. Meanwhile, the proposed model performed better in adaptability to complex terrain, long-term series stability, and disaster response sensitivity.

Conclusion

This research constructed an ECO quality evaluation model through MSRS technology and PCA method, which combined remote sensing images to obtain the required component index data and couple the four index information of greenness, wetness, dryness, and heat to obtain the weight values of different component indicators. The ECO quality level was evaluated according to the size of the index value. Compared with the traditional habitat status index (EI), RSEI had the advantages of obtaining corresponding index factors more conveniently and objectively and played a positive role in evaluating ECO quality. The effectiveness of the proposed model was verified by combining case test analysis. However, the driving factors considered in this study were limited with only meteorological factors, topographic factors, soil factors, land use types among natural factors, and relative wetness and solar radiation intensity. In future, more factors including socio-economic factors, grain output, secondary industry output value, *etc*. should be considered to analyze the impact of driving factors on ECO quality more deeply.

Acknowledgements

This study was supported by Shaanxi Fashion Engineering University Student Innovation and Entrepreneurship Fund 2025 for the project of “GreenView Smart Patrol — Urban Green Space Health Diagnosis System Based on Computer Vision and Machine Learning” (Grant No. S202513125034).

References

1. Li Y, Wang S. 2024. Exploration of eco-environment and urbanization changes based on multi-source remote sensing data — A case study of Yangtze River Delta urban agglomeration. Sustainability. 16(14):5903-5915.
2. Shi F, Li M. 2021. Assessing land cover and ecological quality changes under the new-type urbanization from multi-source remote sensing. Sustainability. 13(21):11979-11989.
3. Cao S, Hu X, Wang Y, Chen C, Xu D, Bai T. 2023. Understanding spatial-temporal interactions of ecosystem services and their drivers in a multi-scale perspective of Miluo using multi-source remote sensing data. Remote Sens. 15(14):3479-3490.
4. Jia X, Jin Z, Mei X, Wang D, Zhu R, Zhang X, *et al*. 2023. Monitoring and effect evaluation of an ecological restoration project using multi-source remote sensing: A case study of Wuliangsuhai watershed in China. Land. 12 (2):349-360.
5. Hong F, He G, Wang G, Zhang Z, Peng Y. 2023. Monitoring of land cover and vegetation changes in Juhugeng Coal mining area based on multi-source remote sensing data. Remote Sens. 15(13):3439-3450.
6. Liu X, Zheng C, Wang G, Zhao F, Tian Y, Li H. 2024. Integrating multi-source remote sensing data for forest fire risk assessment. Forests. 15 (11):2028-2040.
7. Wang Q, Gao M, Zhang H. 2022. Agroecological efficiency evaluation based on multi-source remote sensing data in a typical county of the Tibetan Plateau. Land. 11(4):561-575.
8. Liu X, Li H, Wang S, Liu K, Li L, Li D. 2023. Ecological security assessment of “Grain-for-Green” program typical areas in Northern China based on multi-source remote sensing data. Remote Sens. 15(24):5732-5742.
9. Wu S, Cao L, Xu D, Zhao C. 2023. Historical eco-environmental quality map in China with multi-source data fusion. Appl Sci. 13(14):8051-8066.
10. Tian Y, Wu Z, Li M, Wang B, Zhang X. 2022. Forest fire spread monitoring and vegetation dynamics detection based on multi-source remote sensing images. Remote Sens. 14(18):4431-4444.
11. He K, Fan C, Zhong M, Cao F, Wang G, Cao L. 2023. Evaluation of habitat suitability for Asian elephants in Sipsongpanna under climate change by coupling multi-source remote sensing products with MaxEnt model. Remote Sens. 15(4):1047-1060.
12. Duan H, Yao X, Zhang DH, Jin H, Wei Q. 2022. Long-term temporal and spatial monitoring of cladophora blooms in Qinghai Lake based on multi-source remote sensing images. Remote Sens. 14(4):853-866.
13. Yang J, Xin ZB, Huang Y, Liang X. 2023. Multi-source remote sensing data shows a significant increase in vegetation on the Tibetan Plateau since 2000. Prog Phys Geog. 47(4):597-624.
14. Wang Y, Liu H, Sang L, Wang J. 2022. Characterizing forest cover and landscape pattern using multi-source remote sensing data with ensemble learning. Remote Sens. 14(21):5470-5484.
15. Xu D, Cheng J, Xu S, Geng J, Yang F, Fang H, *et al*. 2022. Understanding the relationship between China’s eco-environmental quality and urbanization using multisource remote sensing data. Remote Sens. 14(1):198-210.
16. Ghorbanian A, Ahmadi SA, Amani M, Mohammadzadeh A, Jamali S. 2022. Application of artificial neural networks for mangrove map using multi-temporal and multi-source remote sensing imagery. Water. 14(2):244-255.
17. Duan D, Sun X, Liang S, Sun J, Fan L, Chen H, *et al*. 2022. Spatiotemporal patterns of cultivated land quality integrated with multi-source remote sensing: A case study of Guangzhou, China. Remote Sens. 14(5):1250-1265.
18. Ren Y, Liu X, Zhang B, Chen X. 2023. Sensitivity assessment of land desertification in China based on multi-source remote sensing. Remote Sens. 15(10):2674-2688.
19. Tang Z, Xia XS, Huang YH, Lu Y, Guo Z. 2022. Estimation of national forest aboveground biomass from multi-source remotely sensed dataset with machine learning algorithms in China. Remote Sens. 14 (21):5487-5499.
20. Li X, Pang Z, Xue F, Ding J, Wang J, Xu T, et al. 2024. Analysis of spatial and temporal variations in evapotranspiration and its driving factors based on multi-source remote sensing data: A case study of the Heihe River Basin. Remote Sens. 16(15):2696-2707.